

RESEARCH ARTICLE

Differential requirements for the Eps15 homology domain proteins EHD4 and EHD2 in the regulation of mammalian ciliogenesis

Tyler Jones¹ | Naava Naslavsky¹ | Steve Caplan^{1,2} 

¹Department of Biochemistry and Molecular Biology, University of Nebraska Medical Center, Omaha, Nebraska, USA

²Fred and Pamela Buffett Cancer Center, University of Nebraska Medical Center, Omaha, Nebraska, USA

Correspondence

Steve Caplan, Department of Biochemistry and Molecular Biology, University of Nebraska Medical Center, Omaha, NE 68198, USA.
Email: scaplan@unmc.edu

Funding information

National Institutes of Health, Grant/Award Numbers: R01GM123557, R01GM133915

Abstract

The endocytic protein EHD1 controls primary ciliogenesis by facilitating fusion of the ciliary vesicle and by removal of CP110 from the mother centriole. EHD3, the closest EHD1 paralog, has a similar regulatory role, but initial evidence suggested that the other two more distal paralogs, EHD2 and EHD4 may be dispensable for ciliogenesis. Herein, we define a novel role for EHD4, but not EHD2, in regulating primary ciliogenesis. To better understand the mechanisms and differential functions of the EHD proteins in ciliogenesis, we first demonstrated a requirement for EHD1 ATP-binding to promote ciliogenesis. We then identified two sequence motifs that are entirely conserved between EH domains of EHD1, EHD3 and EHD4, but display key amino acid differences within the EHD2 EH domain. Substitution of either P446 or E470 in EHD1 with the aligning S451 or W475 residues from EHD2 was sufficient to prevent rescue of ciliogenesis in EHD1-depleted cells upon reintroduction of EHD1. Overall, our data enhance the current understanding of the EHD paralogs in ciliogenesis, demonstrate a need for ATP-binding and identify conserved sequences in the EH domains of EHD1, EHD3 and EHD4 that regulate EHD1 binding to proteins and its ability to rescue ciliogenesis in EHD1-depleted cells.

KEYWORDS

ATP-binding, ciliary vesicle, ciliogenesis, CP110, distal appendage vesicle, EHD1, EHD2, EHD3, EHD4, MICAL-L1, mother centriole, primary cilium, SNAP29

1 | INTRODUCTION

Primary cilia are non-motile organelles involved in hedgehog signaling¹ and other signaling pathways that control key cellular events, including differentiation, tissue homeostasis, apoptosis and cell migration.^{2,3} Initially thought to be motile and later considered vestigial in nature, the primary cilium is an organelle that emanates from the mother centriole (m-centriole) as a microtubule-based axoneme that forms a surrounding ciliary membrane before extending into the

plasma membrane.⁴ The axoneme, a rod-like structure composed of nine microtubule doublets arranged in a circular formation, begins developing between the m-centriole and the ciliary vesicle (CV). Eventually, the CV fuses with the plasma membrane to form the ciliary membrane, a dense region of the membrane that sheaths the protruding axoneme and is home to various receptors and other proteins involved in signal transduction.

Given its role in signaling, it is not surprising that impaired primary cilium biogenesis and/or function can lead to a variety of disease

This is an open access article under the terms of the [Creative Commons Attribution-NonCommercial-NoDerivs](https://creativecommons.org/licenses/by-nc-nd/4.0/) License, which permits use and distribution in any medium, provided the original work is properly cited, the use is non-commercial and no modifications or adaptations are made.

© 2022 The Authors. *Traffic* published by John Wiley & Sons Ltd.

states aptly named ciliopathies.^{5,6} Defective cilio-regulatory genes in mammals can have wide-ranging effects from retinal dystrophy and anosmia⁷ to congenital heart defects, renal cystic disease and numerous developmental disorders.⁸ Accordingly, it is imperative to elucidate the underlying mechanisms responsible for the formation and maintenance of the primary cilium.

The formation of the primary cilium is a closely regulated, step-wise process that only occurs in non-mitotic cells. There are two distinct pathways for ciliogenesis, likely dependent on the cell or tissue type.^{4,9} The extracellular pathway, which is often observed in epithelial cells, occurs when the m-centriole docks directly with the plasma membrane followed by recruitment of regulatory proteins and the subsequent axonemal growth deforms the membrane and extends it into a primary cilium.¹⁰ However, it has been demonstrated recently that a CV is generated in some cell types in the extracellular pathway without extending to form an elongated ciliary membrane in the cytoplasm.¹¹ In the intracellular pathway, common in non-polarized cells, the distal appendages of the m-centriole serve as docking sites for incoming preciliary vesicles from the endocytic pathways which then subsequently fuse to form the CV.¹² The ciliary axoneme begins to extend and migrate within the cell until it fuses with the plasma membrane and forms the primary cilium.¹³ Indeed, disruption of any of these processes leads to impaired ciliogenesis and resulting ciliopathies.

In recent years, it has become clear that endocytic membrane trafficking is essential for the regulation of the intracellular ciliogenesis pathway. One of the initial steps in ciliogenesis is the docking of preciliary vesicles on the distal appendages of the m-centriole, which is mediated by Myosin-Va (MYO5A), an actin-based motor protein that also mediates trafficking of secretory vesicles from the Golgi to the plasma membrane.¹¹ Another endocytic protein, EHD1, with well-documented roles in endosomal fission and receptor recycling^{14–17} and in the regulation of centrosome duplication,^{18,19} is recruited to the centrosome through an interaction with the scaffolding protein, MICAL-L1.²⁰ Both EHD1 and MICAL-L1 interact with Syndapin/PACSIN proteins,^{21–25} F-BAR-containing proteins that have been recently implicated in membrane bending and tubulation and are required for generation of the primary cilium.²⁶ Upon recruitment, EHD1 is then able to coordinate the recruitment of the SNARE protein SNAP29 and both facilitate the removal of the centriolar capping protein CP110 from the m-centriole by a poorly understood mechanism and allow fusion of preciliary vesicles to form the CV.¹³ This in turn leads to a “Rab cascade” in which ARL13b and RAB11 at the ciliary membrane^{1,27} affect the recruitment of RABIN8, thus activating RAB8 and promoting the later steps of ciliogenesis.²⁸ However, it remains unclear precisely how EHD1 regulates ciliogenesis, and in particular how it influences both SNAP29 recruitment and the subsequent removal of CP110 from the m-centriole.

In addition to EHD1, its closest paralog, EHD3 (86% identical by amino acid sequence), has also been implicated in ciliogenesis in mammals and zebrafish.¹³ EHD1 and EHD3 belong to a family of four mammalian EHD proteins that display ~65%–86% amino acid identity. EHD4 hetero-oligomerizes with EHD1 and appears to partially

overlap in function with EHD1 and EHD3 in endosomal regulation.^{29,30} EHD2, the most disparate EHD protein family member, binds to phosphatidylinositol(4,5)-bisphosphate, localizes to the plasma membrane,^{31–33} and is involved in caveolae stabilization.^{34,35} Despite the crucial roles of both EHD1 and EHD3 in the regulation of primary ciliogenesis, initial studies using the human RPE-1 cells suggested that both EHD2 and EHD4 may be dispensable for mammalian primary ciliogenesis.^{13,36–38}

Herein, we describe a novel role for EHD4, but not EHD2 in the regulation of primary ciliogenesis in mouse NIH3T3 cells. We show that EHD1 ATP-binding/hydrolysis is a requirement for ciliogenesis, as substitution of glycine 65, a key conserved residue for ATP-binding and EHD function led to an inability of the mutant protein to rescue ciliogenesis defects in EHD1-depleted cells. To understand why EHD2 is the sole EHD paralog that neither localizes to the primary cilium nor is required for ciliogenesis in NIH3T3 cells, we examined two stretches of amino acids within the EH domain that are 100% conserved between the three EHD proteins that regulate ciliogenesis (EHD1, EHD3 and EHD4), but display key residue differences in EHD2. Indeed, a single residue substitution in EHD1 from glutamate to tryptophan at position 470 (EHD2 contains tryptophan at the residue aligning with EHD1 E470) was sufficient to impair association with the centrosome/centrioles and prevent the mutant protein from rescuing ciliogenesis defects in EHD1-depleted cells. Overall, our study helps to better define the function of EHD proteins in primary ciliogenesis.

2 | MATERIALS AND METHODS

2.1 | Cell lines

NIH3T3 (ATCC; CRL-1658) parental cells, CRISPR/Cas9 gene-edited NIH3T3 cells expressing endogenous levels of EHD2 with GFP attached to the C-terminus, CRISPR/Cas9 gene-edited EHD1 knock-out cells and CRISPR/Cas9 gene-edited EHD4 knock-out cells have been previously described.^{19,39} NIH3T3 cells were cultured at 37°C in 5% CO₂ in DMEM/high glucose (HyClone; SH30243.01) containing 10% heat-inactivated Fetal Bovine Serum (Atlanta Biologicals; S1150), 1X Penicillin Streptomycin (Gibco; 15140-122), 50 mg of Normocin (InvivoGen; NOL-40-09) and 2 mM L-Glutamine (Gibco; 25030-081). RPE cells were cultured at 37°C in 5% CO₂ in DME/F-12 (HyClone; SH30023.01) containing 10% heat-inactivated fetal bovine serum (Atlanta Biologicals; S1150), 1X Penicillin Streptomycin (Gibco; 15140-122), 50 mg of Normocin, 2 mM MEM non-essential amino acids (Gibco; 2301967) and 2 mM L-glutamine. All cell lines were routinely tested for mycoplasma infection.

2.2 | Antibodies

The following antibodies were used (also see Table 1): Rabbit anti-EHD1 (Abcam, ab109311), rabbit anti-EHD4,²⁹ Rabbit anti-acetyl-

TABLE 1 List of antibodies used in this study

Target	Source	Manufacturer	Product ID
ARL13B	Rabbit	ProteinTech	177711-1-AP
EHD1	Rabbit	Abcam	Ab109311
EHD4	Rabbit	Made in-house	Reference 29
Acetylated- α -tubulin (Lys40) (D20G3)	Rabbit	Cell Signaling	5335
Acetylated tubulin	Mouse	Sigma-Aldrich	T7451
CP110	Rabbit	ProteinTech	12780-1-AP
GFP	Mouse	Roche	11814460001
Pan actin	Mouse	Novus	NB600-535
GAPDH(-HRP)	Mouse	ProteinTech	HRP-60004
Mouse(-HRP)	Donkey	Jackson	715-035-151
Rabbit IgG light chain (HRP)	Mouse	Jackson	211-032-171
DAPI	-	Molecular Probes	D1306
GFP(biotin-conjugated)	Goat	Rockland	600-106-215
Streptavidin (Alexa-fluor 488-conjugated)	-	Molecular Probes	S11223
Mouse (Alexa-fluor 488-conjugated)	Goat	Molecular Probes	A11029
Rabbit (Alexa-fluor 568-conjugated)	Goat	Molecular Probes	A11036
Mouse (Alexa-fluor 568-conjugated)	Goat	Molecular Probes	A11031
Rabbit (Alexa-fluor 633-conjugated)	Goat	Molecular Probes	A21070

α -tubulin (Lys40) (D20G3) (Cell Signaling, 5335), mouse anti-acetylated tubulin (Sigma-Aldrich, T7451), rabbit anti-CP110 (ProteinTech, 12780-1-AP), rabbit anti-ARL13B (ProteinTech, 17711-1-AP), mouse anti-GFP (Roche, 11814460001), mouse anti-pan actin (Novus, NB600-535), mouse anti-GAPDH-HRP (ProteinTech, HRP-60004), donkey anti-mouse-HRP (Jackson, 715-035-151), mouse anti-rabbit IgG light chain-HRP (Jackson, 211-032-171), DAPI (4',6-diamidino-2-phenylindole, dihydrochloride) (Molecular Probes, D1306), biotin-conjugated goat anti-GFP (Rockland, 600-106-215), Alexa-fluor 488-conjugated streptavidin (Molecular Probes, S11223), Alexa-fluor 488-conjugated goat anti-mouse (Molecular Probes, A11029), Alexa-fluor 568-conjugated goat anti-rabbit (Molecular Probes, A11036), Alexa-fluor 568-conjugated goat anti-mouse (Molecular Probes, A11031), Alexa-fluor 633-conjugated goat anti-rabbit (Molecular Probes, A21070).

2.3 | DNA constructs, cloning and site-directed mutagenesis

Cloning of EHD1 G65R into the GFP-myc vector was described previously.^{15,40} Cloning of PTD1, EHD1, EHD2, EHD3, EHD4, MICAL-L1 and SNAP29 in the yeast two-hybrid vector pGADT7 and cloning of PVA3, EHD1, EHD2, EHD3 and EHD4 in the yeast two-hybrid vector pGBKT7 were described previously.^{22,29,40} The following constructs were generated via site-directed mutagenesis using QuickChange Site-Directed Mutagenesis Kit (Agilent; 200519) according to the manufacturer's protocol: GFP-myc-EHD1 P446S, GFP-myc-EHD1 E470W, GFP-myc-EHD1 P446S/E470W, pGADT7-EHD1 P446S, pGADT7-EHD1 E470W and pGADT7-EHD1 P446S/E470W.

2.4 | Yeast two-hybrid assay

AH109 yeast was cultured overnight in YPD media containing 10 g/L Bacto Yeast Extract (BD; Ref. 212750), 20 g/L Peptone (Fisher Scientific; CAS RN: 73049-73-7, BP1420-500) and 20 g/L Dextrose (Fisher Scientific; CAS RN: 50-99-7, BP350-1) at 30°C and 250 RPM. Cultures were then spun down at 975g for 5 min and the supernatant was aspirated. Pellets were rinsed with autoclaved MilliQ water and centrifuged for an additional 5 min at 975g and the supernatant was aspirated. Pellets were resuspended in a suspension buffer of 80% autoclaved MilliQ water, 10% lithium acetate pH = 7.6 and 10% 10x TE pH = 7.5. Aliquots of 125 μ l from the cell suspension were then incubated each with 600 μ l of PEG solution (40% PEG [CAS RN: 25322-68-3, Prod. Num. P0885], 100 mM lithium acetate pH = 7.6 in TE pH = 7.5). Next, 1 μ l of Yeastmaker Carrier DNA (TaKaRa Cat# 630440) was added to each aliquot, followed by 1 μ g of each respective plasmid and mixed by inverting twice, then by vortexing twice. Mixtures were then incubated at 30°C and 250 RPM for 30 min. Afterward, 70 μ l of DMSO was added to each tube, followed by inverting/mixing twice and mixtures were incubated at 42°C for 1 h. Samples were then placed on ice for 5 min, followed by centrifugation at 22 000g for 30 s. The supernatant was aspirated and the samples were resuspended in 40 μ l of autoclaved MilliQ water. Aliquots of 15 μ l from each sample were then plated and spread on -2 plates (+His) made using 27 g/L DOB Medium (MP; Cat. No. 4025-032), 20 g/L Bacto Agar (BD; Ref. 214 010) and 0.64 g/L CSM-Leu-Trp (MP; Cat. No. 4520012) and incubated at 30°C for 72-96 h. Following the incubation period, three separate colonies from each sample were selected and added to 600 μ l of autoclaved MilliQ water. In a clean cuvette, 500 μ l of the mixture was added to 500 μ l of autoclaved

water and measured using a spectrophotometer at 600 nm. Mixtures were then normalized to 0.100 λ and 15 μ l of each mixture was spotted onto both a -2 plate and a -3 plate (-His) made using 27 g/L DOB Medium, 20 g/L Bacto Agar and 0.62 g/L CSM-His-Leu-Trp (MP; Cat. No. 4530112). Both plates were incubated at 30°C for 72 h and imaged.

2.5 | siRNA treatment

RPE cells, NIH3T3 parental cells, or CRISPR/Cas9 gene-edited NIH3T3 cells expressing endogenous levels of either EHD1-GFP or EHD2-GFP were plated on fibronectin-coated coverslips and grown for 4 h at 37°C in 5% CO₂. The NIH3T3 parental cells and CRISPR/Cas9 gene-edited NIH3T3 cells were cultured in DMEM/high glucose containing 10% heat-inactivated fetal bovine serum, 1X Penicillin Streptomycin, 50 mg of Normocin and 2 mM L-Glutamine. The RPE cells were cultured in DME/F-12 containing 10% heat-inactivated fetal bovine serum, 1X Penicillin Streptomycin, 50 mg of Normocin, 2 mM MEM non-essential amino acids and 2 mM L-Glutamine. The cells were then treated with either human EHD4 siRNA oligonucleotides (Sigma; Custom Oligonucleotide, Seq: GGUACUGCGGUCUACAUdTdT), mouse EHD4 siRNA oligonucleotides #1 (Dharmacon; Custom Oligonucleotide, Seq: GUUCCACUCACUGAAGCCcdTdT), #2 (Dharmacon; Custom Oligonucleotide, Seq: GAGCAUCAGCAUCAUCGACdTdT), #3 (Sigma; Custom Oligonucleotide, Seq: CAGAUACUUACUGGAGCAAAdTdT) #4 (Sigma; Custom Oligonucleotide, Seq: GAAGUACUUCGAGUCUACAdTdT), or mouse EHD2 siRNA oligonucleotides (Dharmacon; Custom Oligonucleotide, Seq: AAGCTGCCTGCATCTTTGCG) for 72 h at 37°C in 5% CO₂ in 1X Opti-MEM 1 containing 12% heat-inactivated fetal bovine serum and 2 mM L-Glutamine using Lipofectamine RNAiMax transfection reagent (Invitrogen; 56531), following the manufacturer's protocol.

2.6 | Transfection

CRISPR/Cas9 gene-edited NIH3T3 EHD1 knock-out cells were plated on fibronectin-coated coverslips and grown for 4 h at 37°C in 5% CO₂ in DMEM/high glucose containing 10% heat-inactivated fetal bovine serum, 1X Penicillin Streptomycin, 50 mg of Normocin and 2 mM L-Glutamine. The cells were then transfected with the respective plasmid for 48 h at 37°C in 5% CO₂ in DMEM/high glucose containing 10% heat-inactivated fetal bovine serum and 2 mM L-Glutamine, using FuGene 6 Transfection Reagent (Promega; E2691), according to the manufacturer's protocol.

2.7 | Immunofluorescence and serum starvation

RPE cells, parental NIH3T3 cells, CRISPR/Cas9 gene-edited EHD1 knock-out NIH3T3 cells, CRISPR/Cas9 gene-edited EHD4 knock-out cells, CRISPR/Cas9 gene-edited NIH3T3 cells expressing endogenous levels of EHD1-GFP, or CRISPR/Cas9 gene-edited NIH3T3 cells

expressing endogenous levels of EHD2-GFP were subjected to serum starvation. Starvation was performed by pre-warming DMEM/high glucose containing 2 mM L-Glutamine to 37°C. Coverslips with treated cells were washed once in 1X PBS and then were added to wells containing the pre-warmed starvation media and incubated at 37°C in 5% CO₂ for either 1 or 24 h. Following starvation, coverslips were washed twice in 1X PBS and were then fixed in either 4% paraformaldehyde (Fisher Scientific; BP531-500) in PBS for 10 min at room temperature or -20°C methanol (Fisher Scientific; A452-4) for 5 min at -20°C. After fixation, cells were rinsed 3 times in 1X PBS and incubated with primary antibody in staining buffer (1X PBS with 0.5% bovine serum albumin and 0.2% saponin) for 1 h at room temperature. Cells were washed three times in 1X PBS, followed by incubation with the appropriate fluorochrome-conjugated secondary antibody diluted in staining buffer for 30 min. Cells were washed three times in 1X PBS and mounted in Fluoromount-G (SouthernBiotech; 0100-01). Z-stack confocal imaging was performed using a Zeiss LSM 800 confocal microscope with a 63x/1.4 NA oil objective. Ten fields of cells from each condition were collected from at least three independent experiments and assessed.

2.8 | Graphical and statistical analysis

NIH ImageJ was used to calculate corrected total cell fluorescence (CTCF), following instructions provided by The Open Lab Book (<https://theolb.readthedocs.io/en/latest/imaging/measuring-cell-fluorescence-using-imagej.html>). Cells expressing a GFP plasmid were outlined using the selection tool. Area, integrated intensity and mean gray value were measured for each individual cell. Background readings were collected as instructed and CTCF was calculated for each individual cell using the following formula: CTCF = integrated density - (area of selected cell \times mean fluorescence of background readings). All statistical analyses were performed with significance using an independent sample two-tailed *t* test under the assumption that the two samples have equal variances and normal distribution using the Vassarstats website (<http://www.vassarstats.net/>), or when comparing multiple samples, with a one-way ANOVA using post-hoc Tukey test for significance (<https://astatsa.com>). To address biological variations between individual tests, we have designed a modified version of the method described by Folks⁴¹ for deriving a "consensus *p*-value" to determine the likelihood that the collection of different test/experiments collectively suggests (or refutes) a common null hypothesis, modified from the Liptak-Stouffer method.⁴² All the graphics were designed using GraphPad Prism 7.

3 | RESULTS

Given the role of both EHD1 and EHD3 in regulating primary ciliogenesis,^{13,20} it was somewhat unexpected that our previous study in RPE-1 cells suggested that both remaining EHD paralogs, EHD4 and EHD2, appeared to be dispensable for primary ciliogenesis.

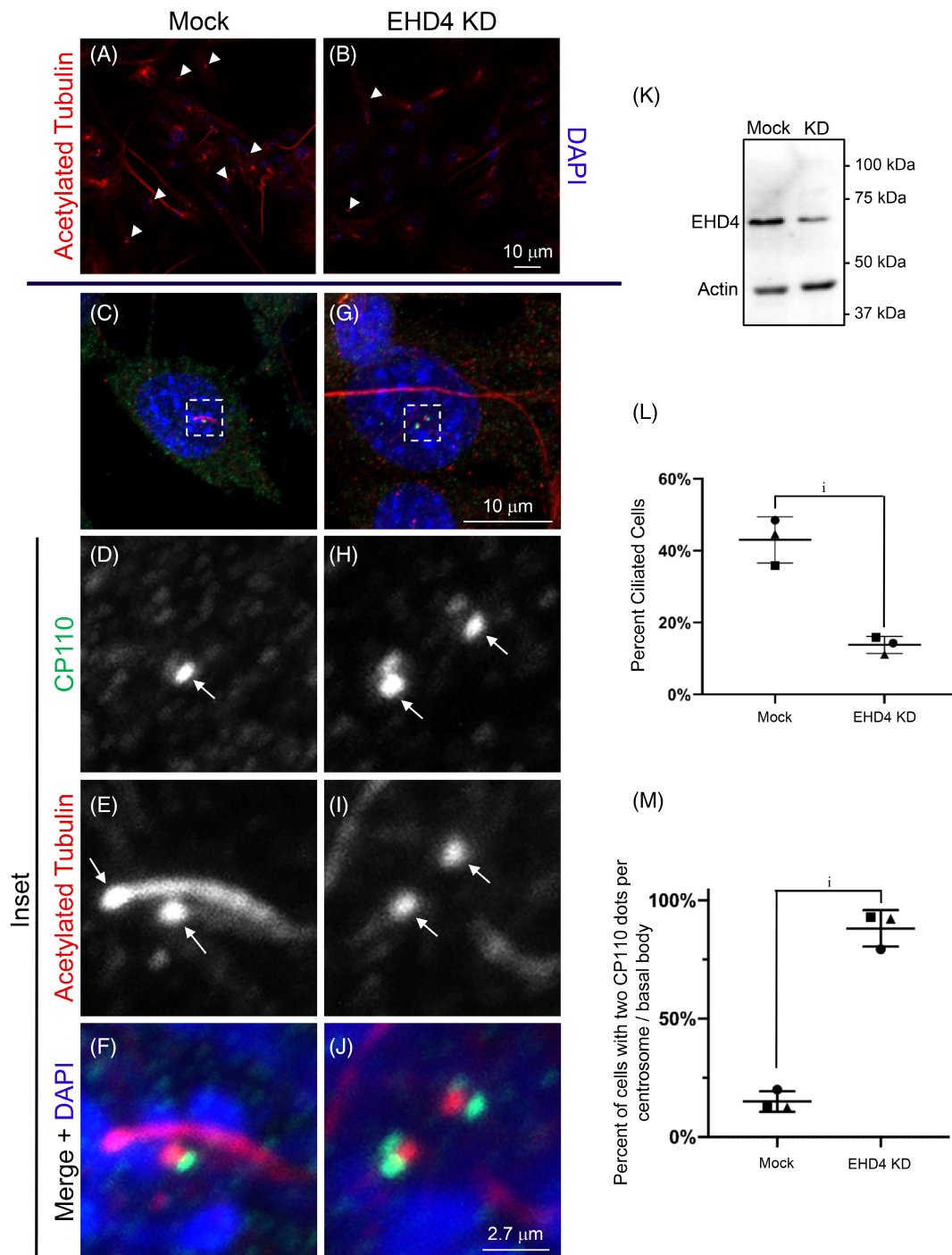


FIGURE 1 EHD4 regulates primary ciliogenesis and its depletion prevents CP110 removal from the m-centriole. (A, B) Representative fields of cells depicting primary cilia labeled with acetylated tubulin (red) and DAPI (blue) in mock-treated (A) and EHD4 knock-down cells (B). (C–J) Representative micrographs depicting primary cilia labeled with acetylated tubulin (red) and marked by CP110 (green) and DAPI (blue) in mock-treated (C–F) and EHD4 knock-down cells (G–J). NIH3T3 cells were either mock-treated with transfection reagent (A; C, inset in D–F), or transfected with EHD4 siRNA oligonucleotides (B; G, inset in H–J) for 48 h, fixed and immunostained with DAPI and antibodies to detect acetylated tubulin and CP110 prior to imaging. Arrowheads denote primary cilia and arrows mark centrosomes/basal bodies in the micrographs. (K) Validation of EHD4 siRNA efficacy by immunoblot analysis, with actin used as a control. (L) Graph depicting the percentage of ciliated cells in mock-treated and EHD4 knock-down cells. (M) Graph illustrating the percentage of centrosomes/basal bodies with two CP110 dots in mock-treated and EHD4 knock-down cells. Error bars denote standard deviation, and *p* values for each experiment were determined by an independent two-tailed *t* test. Percentage of ciliated cells and percentage of cells with two CP110 dots per centrosome/basal body were calculated from two separate sets of three experiments. All six experiments rely on data from 10 images and each experiment is marked by a distinct shape on the graph. Significance between samples for each set of three experiments was calculated by deriving a consensus *p* value based on Folks⁴¹ and Rice⁴² and our previous study³⁰ (see Section 2). Micrographs are representative orthogonal projections from three independent experiments, with 10 sets of z-stacks collected for each treatment per experiment. Bars (B and G), 10 μ m, Bar for insets, 2.7 μ m. *i*: consensus *p* < 0.00001

Whereas EHD2 is an “outlier” with the least sequence identity and functional homology within the EHD-family proteins,³⁷ EHD4 coordinates endosomal fission and recycling through its interactions with EHD1^{29,30} and thus we initially chose to more extensively evaluate its potential role in regulating generation of the primary cilium.

Because our previous study used RPE-1 cells (see also Figure S1), this time we elected to use mouse NIH3T3 cells by first examining

mock-transfected cells (Mock) and comparing them to cells transfected with siRNA oligonucleotides to deplete EHD4 (EHD4 KD). As demonstrated, EHD4-siRNA oligonucleotides significantly decreased EHD4 expression (Figure 1K). In these NIH3T3 cells, we determined the percentage of cells with primary cilia (marked by acetylated tubulin) following serum starvation (Figure 1A,B; quantified in L). While mock-transfected cells displayed approximately 43% ciliation, there

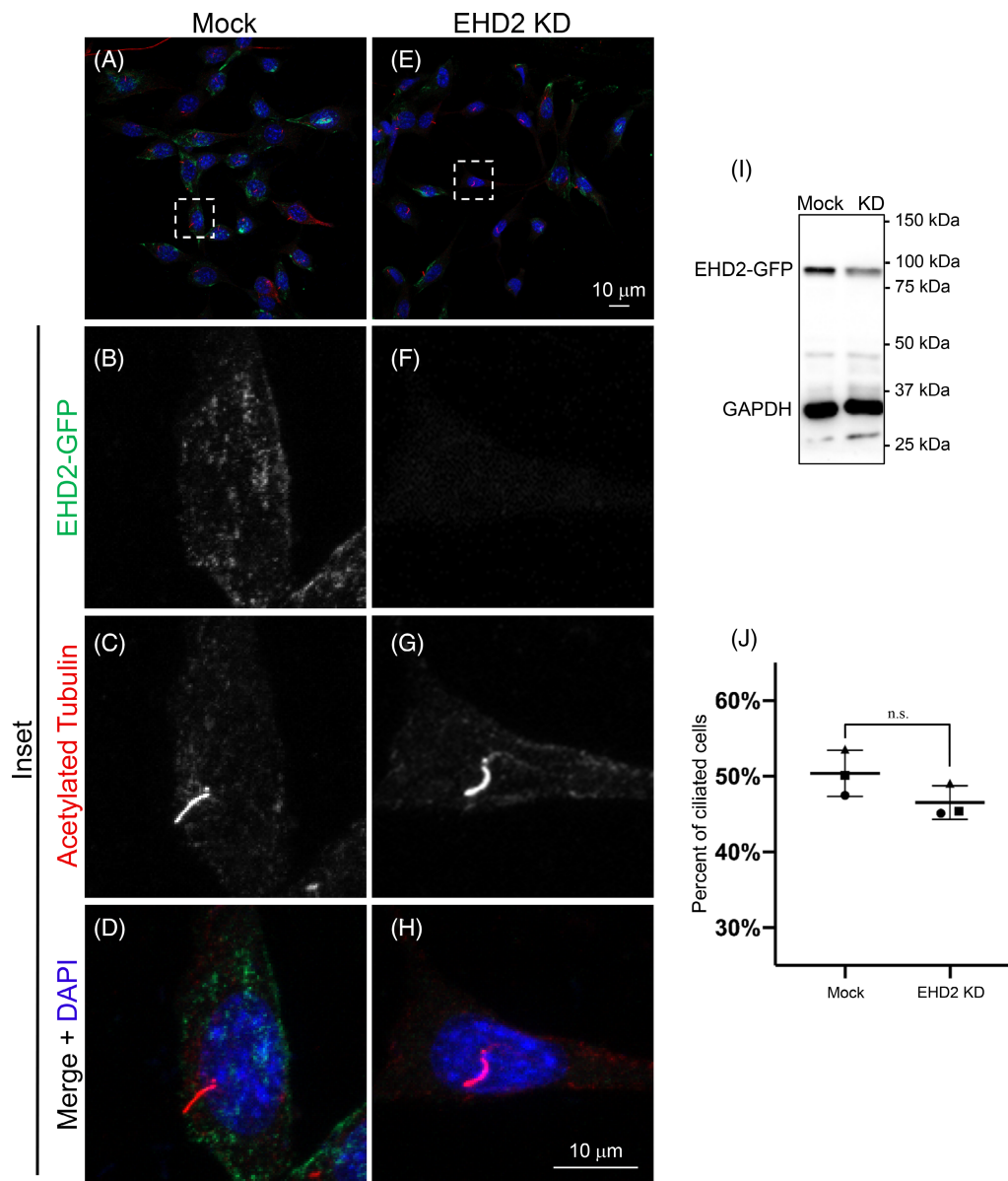


FIGURE 2 EHD2 is not required for normal primary ciliogenesis. (A–H) Representative micrographs of NIH3T3 cells that were engineered by CRISPR/Cas9 to express endogenous levels of EHD2 tagged with GFP (EHD2-GFP) depicting primary cilia labeled with antibodies against acetylated tubulin (red) and DAPI stain (blue). CRISPR/Cas9 gene-edited NIH3T3 EHD2-GFP cells were either mock-treated with transfection reagent (A, inset in B–D), or transfected with EHD2 siRNA (E, inset in F–H) for 48 h, fixed and immunostained with DAPI and an acetylated tubulin antibody prior to imaging. (I) Validation of EHD2 siRNA efficacy by immunoblot analysis. (J) Graph depicting the percentage of ciliated cells in mock-treated and EHD2 knock-down NIH3T3 EHD2-GFP cells. Error bars denote standard deviation and *p* values for each experiment were determined by an independent two-tailed *t* test. All three experiments rely on data from 10 images and each experiment is marked by a distinct shape on the graph. A consensus *p* value was then derived as described previously to assess significant differences between samples from the three experiments. Micrographs are representative orthogonal projections from three independent experiments, with 10 sets of z-stacks collected for each treatment per experiment. Bars, 10 μ m. n.s. = not significant (consensus *p* > 0.05)

was more than a threefold decrease in ciliation in the absence of EHD4 (Figure 1L). Moreover, similar results were observed when NIH3T3 cells were serum starved and immunostained with both acetylated tubulin and the specific ciliary marker, ARL13B (Figure S2). Indeed, antibodies to both markers colocalized on primary cilia of the parental NIH3T3 serum-starved cells (Figure S2A–C and insets, D–F), whereas very few cilia were observed with these markers in EHD4 knock-out (KO) cells (Figure S2G–I and insets, J–L). Quantification revealed an almost fivefold decrease in ciliation marked by ARL13B in the EHD4 KO cells compared to the parental NIH3T3 cells (Figure S2M with EHD4 knock-out cells validated in Figure S2N). Moreover, four different EHD4 oligonucleotides (from two different companies) led to an approximately threefold decrease in the percentage of ciliated NIH3T3 cells compared to mock-treated cells (Figure S2O, knock-down efficacy shown in Q). In addition, a modest but significant decrease in EHD1 localization to the cilium or centrosome was observed upon EHD4 depletion, implicating EHD4 partially in control of EHD1 recruitment (Figure S2P). These results led us to conclude that EHD4 likely regulates primary ciliogenesis in NIH3T3 cells, potentially in a similar manner to EHD1 or in part through its recruitment of EHD1.

EHD1 localizes to the primary cilium, interacts with the SNARE protein SNAP29 to facilitate fusion of distal appendage vesicles and is required for the removal of centriolar capping protein CP110 from the m-centriole, a key early step in primary cilium biogenesis.¹³ Similar to EHD1, EHD4 could be observed at the centriole(s) or along the primary cilium of NIH3T3 cells in about 43% of cells (standard deviation ~14%) (Figure S3). Accordingly, we next asked whether EHD4 is required for CP110 removal. Cells were either mock-transfected (Figure 1C and insets D–F) or transfected with EHD4 siRNA oligonucleotides (Figure 1G and insets H–J), and the percentage of cells

containing two CP110 dots per centrosome/basal body after serum starvation was calculated for mock- and siRNA-transfected cells. As illustrated in the micrographs (Figure 1C,G) and quantified in the graph (Figure 1M), whereas only about 20% of mock-transfected cells retained CP110 on the centrosome/basal body, ~90% of EHD4-depleted cells maintained CP110 on the centrosome/basal body. These results indicate a role for EHD4 in the removal of CP110 from the centrosome/basal body.

Our data now support a role for EHD4 in primary ciliogenesis, leaving EHD2 as the sole EHD paralog whose role in cilia biogenesis appears to be dispensable. EHD2 shares the least sequence identity with its paralogs,³⁸ and is the only EHD protein that localizes to the plasma membrane.^{31,32} To further address whether EHD2 regulates primary ciliogenesis, we took advantage of recently engineered CRISPR/Cas9 gene-edited NIH3T3 cells that express EHD2-GFP at endogenous levels, allowing us to easily monitor knock-down efficacy.^{19,39} These cells were generated from parental NIH3T3 cells and the C-terminal GFP tag was confirmed to not affect EHD2 localization or function, consistent with other studies on EHD paralogs.^{39,43} Use of this cell line expressing EHD2-GFP at endogenous levels facilitates more robust detection of EHD2 in our system. NIH3T3 EHD2-GFP cells were subjected to either mock-siRNA transfection (Figure 2A and insets B–D) or knock-down with EHD2 siRNA oligonucleotides (Figure 2E and insets F–H), and reduced EHD2-GFP expression was confirmed by immunoblotting (Figure 2I). Primary cilia were marked by immunostaining with acetylated tubulin, and the number of mock-treated and knock-down cells that generated primary cilia was counted (Figure 2A,E; quantified in J). As shown, approximately 50% of mock-treated cells expressing endogenous EHD2-GFP generated primary cilia, and there was no significant difference in the percent of ciliated cells

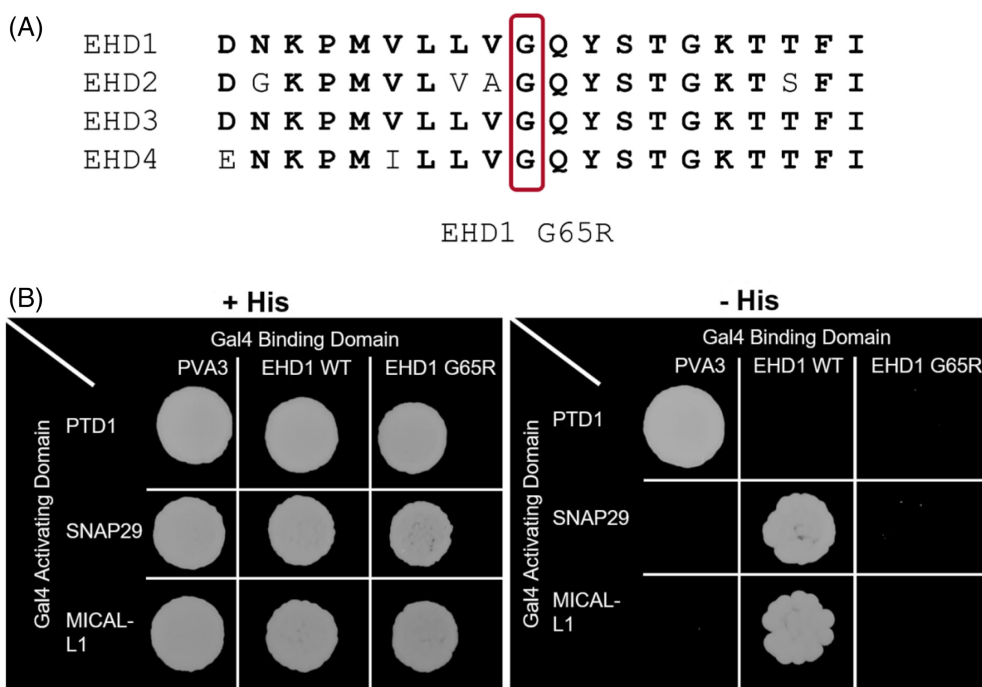


FIGURE 3 The EHD1 G65R mutant does not bind to SNAP29 and MICAL-L1. (A) Amino acid sequence comparison of the four human EHD orthologs, EHD1–4, in the region adjacent to glycine 65. Sequences are aligned with residues 56–75 of EHD1. (B) Yeast two-hybrid colony growth reflecting interactions between either EHD1 WT or EHD1 G65R with SNAP29 and MICAL-L1. The experiment depicted is representative of three independent experiments.

upon EHD2 depletion. Overall, these data suggest that EHD2 is the only EHD protein dispensable for primary ciliogenesis, either in RPE-1 or NIH3T3 cells.

C-terminal EHD proteins have ATPase activity,^{44,45} and a crucial glycine residue (G65) is conserved in all four paralogs (Figure 3A) and is required for EHD1 function in worms and mammalian cells.^{15,46,47}

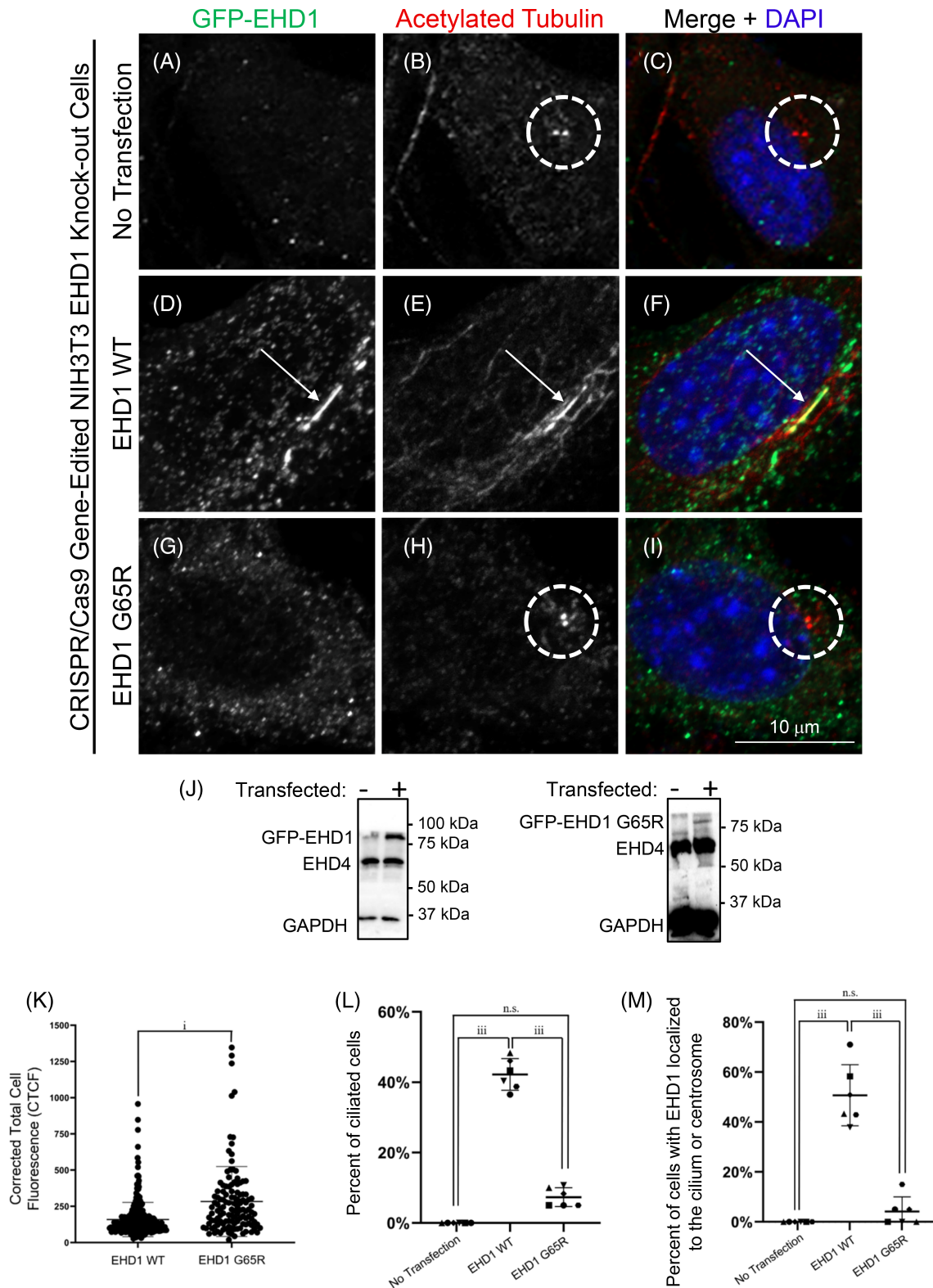


FIGURE 4 Legend on next page.

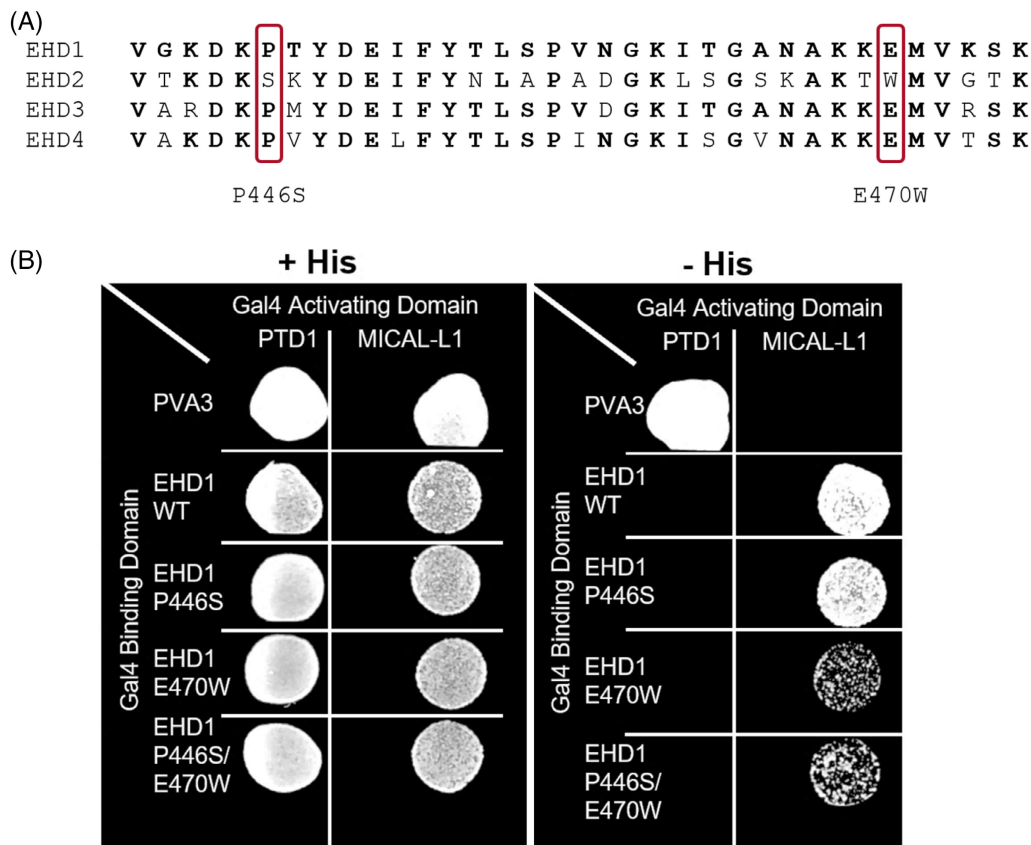


FIGURE 5 EHD1 E470W, but not P446S, disrupts MICAL-L1 binding. (A) Amino acid sequence alignment highlighting residue homology between residues 441 and 475 of EHD1 and its paralogs EHD2, EHD3 and EHD4. Based on these alignments, P446S and E470W substitutions in EHD1 were made to conform with the EHD2 sequences. (B) Yeast two-hybrid colony growth depicting interactions between either EHD1 WT, EHD1 P446S, EHD1 E470W, or EHD1 P446S/E470W with MICAL-L1.

While G65R amino acid substitutions impair EHD1 function in endocytic trafficking and recycling, the potential role of ATP binding and hydrolysis has not been examined in primary ciliogenesis. To address the potential requirement of ATP binding/hydrolysis in primary ciliogenesis, we chose to study EHD1 because it has been the best characterized EHD paralog, especially in ciliogenesis. As demonstrated using a selective yeast two hybrid binding assay, co-transformed yeast with EHD1 G65R and either SNAP29 or MICAL-L1

exhibited a lack of yeast growth on selective plates suggesting perturbed interactions between the ATP-binding EHD1 mutant and both SNAP29 and MICAL-L1 (Figure 3B). Using CRISPR/Cas9 gene-edited NIH3T3 cells lacking EHD1 (EHD1 knock-out), we transfected these cells either with wild-type GFP-EHD1 (Figure 4D-F), with GFP-EHD1 G65R (Figure 4G-I), or we left them untransfected (Figure 4A-C). Transfection of either the correct-size wild-type GFP-EHD1 or GFP-EHD1 G65R was confirmed by immunoblotting

FIGURE 4 Ciliogenesis in EHD1 knock-out cells is rescued by WT EHD1 but not the EHD1 G65R mutant. (A-I) Representative micrographs depicting primary cilia labeled by acetylated tubulin (red) and GFP-EHD1 (green) and DAPI stain (blue) in EHD1 knock-out (KO) cells that were either untransfected, or transfected with GFP-EHD1 WT, or GFP-EHD1 G65R. CRISPR/Cas9 gene-edited NIH3T3 EHD1-KO cells were either mock-treated with transfection reagent (no transfection) (A-C), transfected with GFP-EHD1 WT (D-F), or transfected with the GFP-EHD1 G65R mutant (G-I) for 48 h, fixed and immunostained with DAPI, an anti-GFP antibody and an acetylated tubulin antibody prior to imaging. (J) Validation of GFP-EHD1 WT and G65R transfection efficacy by immunoblot analysis. (K) Graph illustrating the corrected total cell fluorescence values for each cell transfected with either GFP-EHD1 WT or GFP-EHD1 G65R. (L) Graph depicting the percentage of ciliated cells in non-transfected, GFP-EHD1 WT transfected and GFP-EHD1 G65R transfected cells. (M) Graph illustrating the percent of cells where EHD1 is localized to the primary cilium or centrosome in non-transfected, GFP-EHD1 WT transfected and GFP-EHD1 G65R transfected cells. Error bars denote standard deviation, and *p* values for each experiment were determined by one-way ANOVA. All six experiments rely on data from 10 images and each experiment is marked by a distinct shape on the graph. A consensus *p* value was then derived as described previously to assess significant differences between samples from the six experiments. Micrographs are representative orthogonal projections from six independent experiments, with 10 sets of z-stacks collected for each treatment per experiment. Bar, 10 μ m. n.s. = not significant (consensus *p* > 0.05). i: *p* < 0.001; iii consensus *p* < 0.00001

(Figure 4J) and the cells were analyzed by confocal microscopy after serum starvation and immunostaining (Figure 4A-I). As anticipated from previous studies, the N-terminal GFP tag behaved similar to the

C-terminal EHD1-GFP tag and did not impair EHD1 function or localization.^{39,43} Indeed, untransfected EHD1 knock-out cells displayed little ciliation under serum-starved conditions (Figure 4A-C; quantified

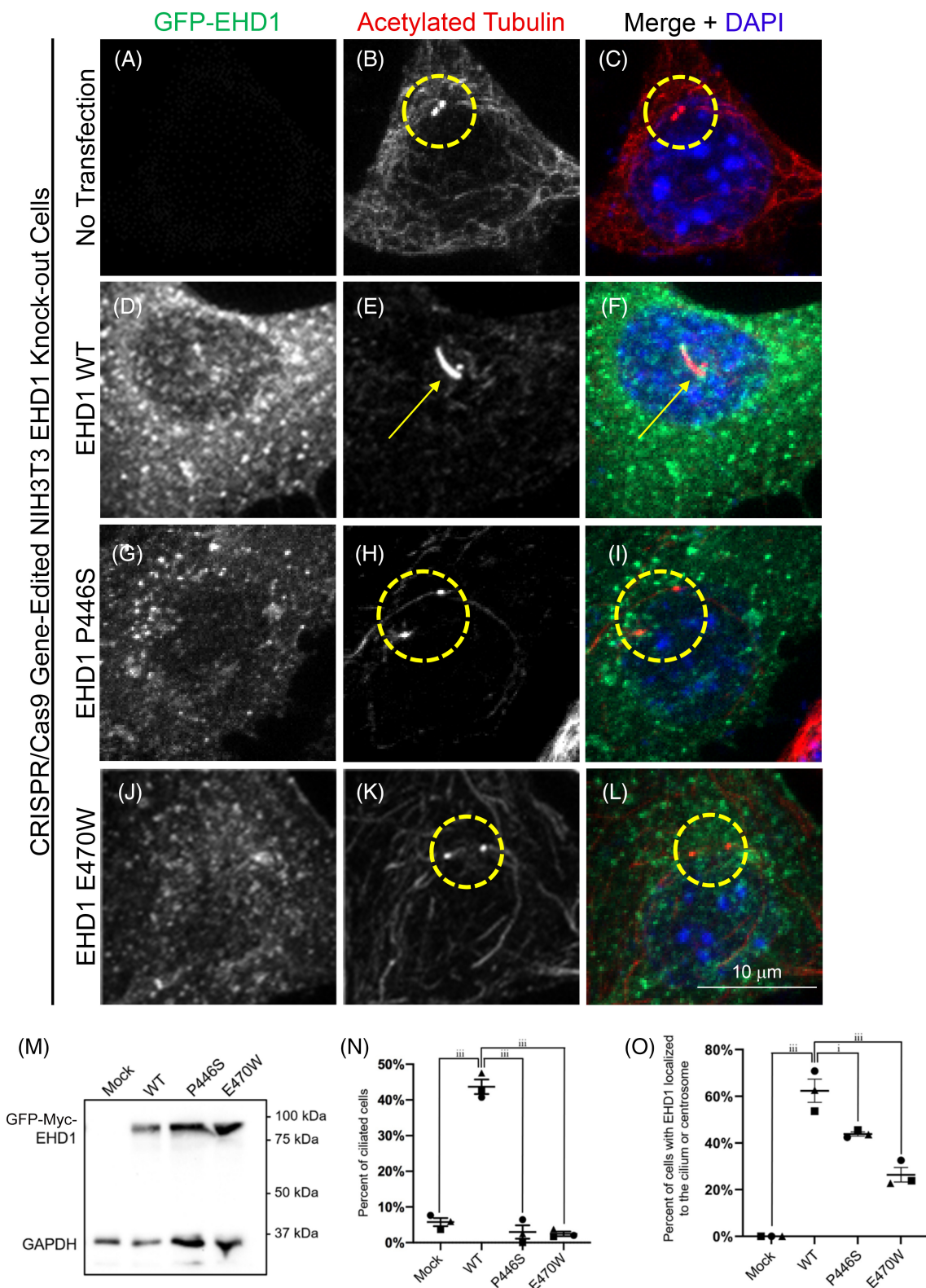


FIGURE 6 Legend on next page.

in L). Our next goal was to transfect WT GFP-EHD1 and the GFP-EHD1 G65R mutant back into EHD1 knock-out cells, to determine whether the mutant EHD1 is capable of rescuing ciliation. However, because wild-type GFP-EHD1 and GFP-EHD1 G65R were globally expressed at different levels as shown by immunoblotting (Figure 4J), and to display significance our analyses must address expression levels on a cell-by-cell basis, we measured corrected total cell fluorescence (CTCF) for individual cells expressing either wild-type GFP-EHD1 or GFP-EHD1 G65R (Figure 4K). As shown, despite lower global levels of transfection, individual cells expressing GFP-EHD1 G65R had a similar (or even slightly higher) mean CTCF than WT GFP-EHD1. Accordingly, because introduction of wild-type GFP-EHD1 increased the percent of ciliated cells to over 50% (Figure 4D–F; quantified in L) whereas introduction of GFP-EHD1 G65R did not (Figure 4G–I; quantified in L), we can conclude that GFP-EHD1 G65R is incapable of rescuing ciliogenesis in knock-out cells. Moreover, whereas ~50% of wild-type GFP-EHD1 could be observed localized to the primary cilium, localization to the cilium was dramatically reduced when GFP-EHD1 G65R was introduced into the cells (Figure 4M). Collectively, these data suggest that EHD1 requires ATP binding and/or hydrolysis for primary ciliogenesis.

The C-terminal EHD paralogs share considerable residue sequence homology, but nonetheless carry out distinct functions,^{17,38} potentially because of subtle differences in their ability to interact with partners via their EH domains.^{33,48–51} Accordingly, we hypothesized that such differences between the EH domains of EHD1 and EHD2 might account for their differential ability to regulate primary ciliogenesis. One potentially significant difference between EHD1 and EHD2 is that EHD1 binds to MICAL-L1 and is recruited to membranes by this interaction, whereas EHD2 displays no interaction with endosomal MICAL-L1 and binds to phosphatidylinositol(4,5)-bisphosphate to localize proximal to the plasma membrane.^{22,24,31} Given the status of EHD2 as the only C-terminal EHD protein that fails to localize to primary cilia and regulate ciliogenesis, we searched for sequences within the EH domain that might distinguish EHD2 from its paralogs (Figure 5A). As illustrated, we identified two locations within the EH domains where a single amino acid displayed 100% identity between EHD1, EHD3 and EHD4, but had a non-conserved residue aligned in the same position for EHD2: proline 446 (in EHD1), is replaced by a serine in EHD2, and glutamate

470 (in EHD1) is substituted by tryptophan in EHD2 (Figure 5A). To address our hypothesis that subtle changes in the EHD2 EH domain modulate its interactions with NPF-containing proteins, and thus alter EHD2 localization and ability to be recruited to endosomes and organelles such as the primary cilium, we instituted substitutions to the highly conserved P446 and E470 in EHD1, rendering them P446S and E470W to mimic the EH domain of EHD2. As demonstrated using a selective yeast two hybrid binding assay, yeast co-transformed with EHD1 E470W and MICAL-L1 displayed significantly diminished growth on plates lacking histidine, suggesting an impaired interaction between the two proteins (Figure 5B). On the other hand, the EHD1 P446S substitution did not affect EHD1 binding to MICAL-L1 in this assay. Consistent with this, double EHD1 substitutions containing both P446S and E470W displayed similar delayed yeast growth/reduced binding to the single EHD1 E470W substitution, further supporting a role for E470 in binding to MICAL-L1, whereas P446 is likely dispensable for this binding.

Because MICAL-L1 is crucial for the recruitment of EHD1 to endocytic membranes,^{22,24} we next asked whether the EHD1 E470W mutant (which displays a weakened interaction with MICAL-L1) can “rescue” ciliogenesis defects when transfected into NIH3T3 CRISPR/Cas9 gene-edited cells lacking EHD1 expression (Figure 6). As demonstrated, in EHD1 knock-out cells that underwent no transfection, serum starvation led to detection of very few ciliated cells (~5%) (Figure 6A–C; quantified in N), whereas transfection of the knock-out cells with wild-type GFP-EHD1 (Figure 6M) increased the percent of ciliated cells expressing wild-type GFP-EHD1 to about 45% (Figure 6D–F; quantified in N). However, when GFP-EHD1 E470W was transfected instead of wild-type GFP-EHD1 in this “rescue” system (Figure 6M), almost no ciliated cells were detected (Figure 6G–I; quantified in N). Surprisingly, despite its ability to bind MICAL-L1 similar to wild-type, the EHD1 P446S mutant was unable to rescue the ciliogenesis defects when transfected into EHD1 knock-out cells (Figure 6J–L,M; quantified in N). However, both E470W and P446S EHD1 mutants displayed significantly reduced localization to the centrosome/centrioles compared to wild-type EHD1 (Figure 6O), suggesting that in addition to maintaining an interaction with MICAL-L1, additional mechanisms may be required for the recruitment of EHD1 and its regulation of primary ciliogenesis.

FIGURE 6 EHD1 P446S and E470W do not rescue ciliogenesis. (A–L) Representative micrographs depicting primary cilia labeled with acetylated tubulin (red), GFP-EHD1 (green) and DAPI stain (blue) in NIH3T3 EHD1-KO cells that were mock-treated (no transfection), or transfected with GFP-EHD1 WT, GFP-EHD1 P446S, or GFP-EHD1 E470W. CRISPR/Cas9 gene-edited NIH3T3 EHD1-KO cells were either mock-treated with transfection reagent (no transfection) (A–C), transfected with GFP-EHD1 WT (D–F), transfected with GFP-EHD1 P446S (G–I), or transfected with GFP-EHD1 E470W (J–L) for 48 h, fixed and immunostained with DAPI, an anti-GFP antibody and an acetylated tubulin antibody prior to imaging. (M) Validation of GFP-EHD1 transfection efficiency by immunoblot analysis. (N) Graph depicting the percentage of ciliated cells in mock-treated, GFP-EHD1 WT, GFP-EHD1 P446S and GFP-EHD1 E470W cells. (O) Graph illustrating the percent of cells with EHD1 localized to the primary cilium or centrosome in mock-treated, GFP-EHD1 WT, GFP-EHD1 P446S and GFP-EHD1 E470W cells. Error bars denote standard deviation and *p* values for each experiment were determined by one-way ANOVA. All three experiments rely on data from 10 images and each experiment is marked by a distinct shape on the graph. A consensus *p* value was then derived as described previously to assess significant differences between samples from the three experiments. Micrographs are representative orthogonal projections from three independent experiments, with 10 sets of z-stacks collected for each treatment per experiment. Bar, 10 μ m. (i) consensus *p* < 0.05, (iii) consensus *p* < 0.00001

4 | DISCUSSION

Ciliogenesis is crucial for the development of mammalian organisms as well as signaling at the cellular level.⁵² While an increasing number of proteins involved in the process of primary ciliogenesis have been identified in recent years, our knowledge of the protein machinery involved, as well as the mechanisms of their action in the regulation of ciliogenesis, remains poorly understood.

A growing number of endocytic regulatory proteins have been identified as modulators of ciliogenesis, notably related to the Rab11-Rab8 cascade.^{28,53,54} More recently, proteins that interact with Rab effectors, such as MICAL-L1²⁰ and EHD1,¹³ have also been implicated in primary ciliogenesis. Of the EHD1 family, both EHD1 and its closest paralog, EHD3, regulate ciliogenesis.¹³ However, despite a significant degree of amino acid identity with EHD1, initial analyses suggested that both EHD4 and EHD2 were dispensable for primary ciliogenesis in RPE-1 cells. The redundancy of EHD1 and EHD3 for ciliogenesis in the human RPE-1 cell line led us to postulate that EHD4, which is almost 75% identical to EHD1 in amino acid sequence, might also be involved in ciliogenesis. Indeed, we demonstrated that expression of EHD4 but not EHD2 is required for primary ciliogenesis in the mouse NIH3T3 cell line. Not only is EHD4 significantly more homologous to EHD1/EHD3 than EHD2, but all three proteins, EHD1, EHD3 and EHD4 can hetero-oligomerize with one

another and all have been ascribed roles at endosomes.³⁸ Although EHD4 depletion has little impact on the expression of the other EHD family proteins,²⁹ its effects on ciliogenesis could be partially mediated by its modest effect on EHD1 localization and recruitment to the centrioles/centrosome (Figure S2P). On the other hand, EHD2 neither hetero-oligomerizes with its EHD paralogs nor does it localize to endosomes or affect their function; EHD2 primarily localizes to the proximity of the plasma membrane and has been linked to caveolae mobility.^{31–35} While the precise mechanism by which EHD1 functions in ciliogenesis remains elusive, EHD1/EHD3 and EHD4 are required for a key step that involves the removal of the capping protein, CP110, from the m-centriole.

The mechanistic roles of EHD1 and the EHD proteins in regulating ciliogenesis remain, at best, partially understood. Although SNAP29 recruitment, fusion and formation of the ciliary vesicle, and the removal of CP110 from the m-centriole all require EHD1 expression,¹³ the manner in which EHD1 mediates these events has not been elucidated. We have now determined that EHD1 ATP-binding and hydrolysis function is required for these key steps of ciliogenesis. Indeed, the EHD1 G65R mutant has a cytoplasmic localization and previous studies have demonstrated that both EHD1 G65R and EHD3 G65R display reduced binding to NPF-containing binding partners as well as impaired hetero- and homo-oligomerization.⁴⁵ Strikingly, EHD1 G65R fails to interact

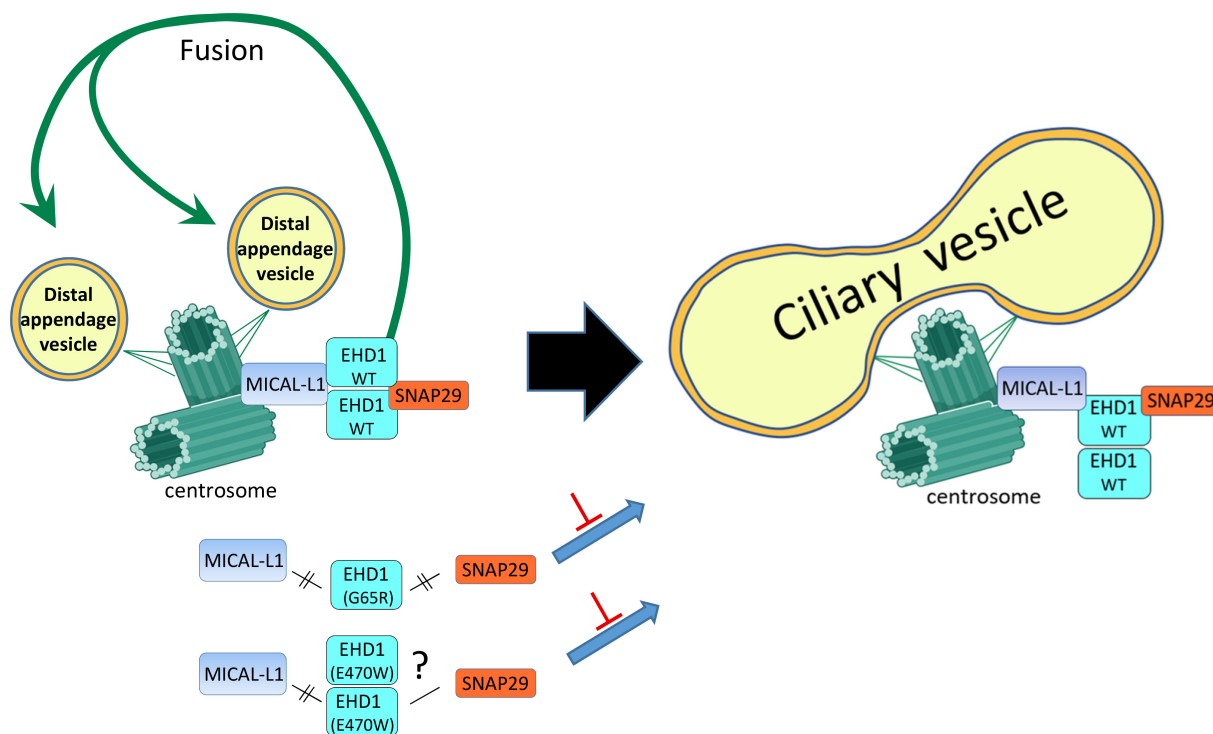


FIGURE 7 Proposed mechanism of SNAP29 recruitment for distal appendage vesicle fusion and ciliary vesicle formation. Model depicting a proposed mechanism by which EHD1 mediates primary ciliogenesis. EHD1 dimers are recruited to the centrosome by MICAL-L1, which in turn recruit SNAP29 to mediate the fusion of the distal appendage vesicles to form the ciliary vesicle. Dimerization of EHD1 may facilitate concomitant interactions of individual EHD1 proteins with the NPF-containing proteins MICAL-L1 and SNAP29. The EHD1 ATP-binding/hydrolysis mutant G65R is unable to dimerize and fails to interact with either MICAL-L1 or SNAP29, preventing fusion of the distal appendage vesicles and formation of the ciliary vesicle. EHD1 E470W exhibits reduced binding to MICAL-L1 and its ability to interact with SNAP29 is currently unknown, but it remains incapable of supporting ciliogenesis.

with SNAP29, suggesting an essential role for ATP-binding/hydrolysis to recruit a SNARE implicated in ciliary vesicle fusion, a key step in early ciliogenesis.

Additional mechanistic information is derived from sequence analysis of the four C-terminal EHD protein EH domains which are crucial for protein-protein interactions. Given that EHD1, EHD3 and EHD4 are all required for primary ciliogenesis in NIH3T3 cells, whereas EHD2 is dispensable, we searched for sequence motifs that were identical in EHD1/3/4 (in human and mouse proteins) but displayed non-conserved residues in EHD2. In mouse and human proteins we observed that: (1) proline 446 (P446) of EHD1 was conserved in EHD3 and EHD4, but was substituted with a serine in EHD2, and (2) glutamate 470 (E470) of EHD1 was conserved in EHD3 and EHD4, but was replaced with tryptophan in EHD2. When we replaced P446 in EHD1 with serine (P446S), we did not observe any discernable difference in binding to MICAL-L1. However, the E470W substitution led to significantly decreased binding between EHD1 and MICAL-L1. Based on our NMR solution structure of the EHD1 EH domain,^{50,51,55} E470 is not in the binding pocket for NPF motifs and is not anticipated to directly contact NPF peptides. However, previous studies have shown that subtle changes in the residues outside the binding pocket can nonetheless influence the ability of the EH domain to interact with binding partners.⁴⁸ These findings may help explain how E470 is required for the recruitment of both EHD1 and EHD3 (and not EHD2) to the centrosome/centrioles to regulate primary ciliogenesis, because this conserved residue may be required for optimal MICAL-L1 binding. However, because wild-type EHD4 only weakly interacts with MICAL-L1,²³ its recruitment and the significance of E470 for this paralog in the regulation of ciliogenesis might rely on another NPF-containing binding partner.

As anticipated, EHD1 E470W not only displays a weakened association with MICAL-L1, thus impairing its recruitment to the centrosome/centrioles, but it also fails to rescue primary ciliogenesis when introduced into EHD1-depleted cells. Surprisingly, the P446S mutant also displays little or no rescue of ciliogenesis in these EHD1 knock-out cells. Because P446 is not required for MICAL-L1 binding, we speculate that there are additional mechanisms by which EHD proteins modulate ciliogenesis. Overall, we have identified a previously unidentified role for EHD4 in the regulation of ciliogenesis, and determined that the more distal paralog, EHD2, is dispensable for the process of ciliary generation. Importantly, we have also shed new light on the mechanisms by which EHD1 and its paralogs regulate ciliogenesis, by demonstrating that ATP-binding/hydrolysis is essential for ciliogenesis and by identifying key residues in the EH domain that are also required, in addition to the previously identified EHD1 K483 and W485 residues that affect tubulovesicular membrane function and protein binding, respectively.¹³ These findings support a model in which ATP-binding/hydrolysis and E470 may be needed for oligomers of EHD1 to bind both MICAL-L1 and SNAP29 (Figure 7). This is likely mediated by interactions of EH domains from distinct EHD1 proteins separately with each binding partner, thus promoting recruitment to the centrosome/centrioles and ciliary vesicle fusion,

respectively (Figure 7). Elucidating the complete mechanisms by which EHD proteins facilitate CP110 removal from the microcentriole remains an important future goal.

ACKNOWLEDGMENTS

The authors would like to acknowledge the National Institute of General Medical Sciences (NIGMS) of the National Institutes of Health (NIH) for the following grant support (R01GM123557 and R01GM133915 to Steve Caplan).

CONFLICTS OF INTEREST

The authors declare that there are no conflicts of interest.

PEER REVIEW

The peer review history for this article is available at <https://publons.com/publon/10.1111/tra.12845>.

ORCID

Steve Caplan  <https://orcid.org/0000-0001-9445-4297>

REFERENCES

1. Caspary T, Larkins CE, Anderson KV. The graded response to sonic hedgehog depends on cilia architecture. *Dev Cell*. 2007;12(5):767-778.
2. Satir P, Pedersen LB, Christensen ST. The primary cilium at a glance. *J Cell Sci*. 2010;123(Pt 4):499-503.
3. Pazour GJ, Witman GB. The vertebrate primary cilium is a sensory organelle. *Curr Opin Cell Biol*. 2003;15(1):105-110.
4. Sorokin S. Centrioles and the formation of rudimentary cilia by fibroblasts and smooth muscle cells. *J Cell Biol*. 1962;15:363-377.
5. Youn YH, Han YG. Primary cilia in brain development and diseases. *Am J Pathol*. 2018;188(1):11-22.
6. Duldulao NA, Li J, Sun Z. Cilia in cell signaling and human disorders. *Protein Cell*. 2010;1(8):726-736.
7. Makelainen S, Hellsand M, van der Heiden AD, et al. Deletion in the Bardet-Biedl syndrome gene TTC8 results in a syndromic retinal degeneration in dogs. *Genes*. 2020;11(9):1090.
8. Reiter JF, Leroux MR. Genes and molecular pathways underpinning ciliopathies. *Nat Rev Mol Cell Biol*. 2017;18(9):533-547.
9. Sorokin SP. Reconstructions of centriole formation and ciliogenesis in mammalian lungs. *J Cell Sci*. 1968;3(2):207-230.
10. Wang L, Dynlacht BD. The regulation of cilium assembly and disassembly in development and disease. *Development*. 2018;145(18):dev151407.
11. Wu CT, Chen HY, Tang TK. Myosin-Va is required for preciliary vesicle transportation to the mother centriole during ciliogenesis. *Nat Cell Biol*. 2018;20(2):175-185.
12. Garcia G 3rd, Raleigh DR, Reiter JF. How the ciliary membrane is organized inside-out to communicate outside-in. *Curr Biol*. 2018;28(8):R421-R434.
13. Lu Q, Insinna C, Ott C, et al. Early steps in primary cilium assembly require EHD1/EHD3-dependent ciliary vesicle formation. *Nat Cell Biol*. 2015;17(4):531.
14. Cai B, Xie S, Caplan S, Naslavsky N. GRAF1 forms a complex with MICAL-L1 and EHD1 to cooperate in tubular recycling endosome vesiculation. *Front Cell Dev Biol*. 2014;2:22.
15. Caplan S, Naslavsky N, Hartnell LM, et al. A tubular EHD1-containing compartment involved in the recycling of major histocompatibility complex class I molecules to the plasma membrane. *EMBO J*. 2002;21(11):2557-2567.

16. Dhawan K, Naslavsky N, Caplan S. Sorting nexin 17 (SNX17) links endosomal sorting to Eps15 homology domain protein 1 (EHD1)-mediated fission machinery. *J Biol Chem.* 2020;295(12):3837-3850.
17. Naslavsky N, Caplan S. The enigmatic endosome - sorting the ins and outs of endocytic trafficking. *J Cell Sci.* 2018;131(13):jcs216499.
18. Naslavsky N, Caplan S. Endocytic membrane trafficking in the control of centrosome function. *Curr Opin Cell Biol.* 2020;65:150-155.
19. Xie S, Reinecke JB, Farmer T, et al. Vesicular trafficking plays a role in centriole disengagement and duplication. *Mol Biol Cell.* 2018;29(22):2622-2631.
20. Xie S, Farmer T, Naslavsky N, Caplan S. MICAL-L1 coordinates ciliogenesis by recruitment of EHD1 to the primary cilium. *J Cell Sci.* 2019;132(22):jcs233973.
21. Giridharan SS, Cai B, Naslavsky N, Caplan S. Trafficking cascades mediated by Rab35 and its membrane hub effector, MICAL-L1. *Commun Integr Biol.* 2012;5(4):384-387.
22. Giridharan SS, Cai B, Vitale N, Naslavsky N, Caplan S. Cooperation of MICAL-L1, syndapin2, and phosphatidic acid in tubular recycling endosome biogenesis. *Mol Biol Cell.* 2013;24(11):1776-1790.
23. Sharma M, Giridharan SS, Rahajeng J, Caplan S, Naslavsky N. MICAL-L1: an unusual Rab effector that links EHD1 to tubular recycling endosomes. *Commun Integr Biol.* 2010;3(2):181-183.
24. Sharma M, Giridharan SS, Rahajeng J, Naslavsky N, Caplan S. MICAL-L1 links EHD1 to tubular recycling endosomes and regulates receptor recycling. *Mol Biol Cell.* 2009;20(24):5181-5194.
25. Braun A, Pinyol R, Dahlhaus R, et al. EHD proteins associate with syndapin I and II and such interactions play a crucial role in endosomal recycling. *Mol Biol Cell.* 2005;16(8):3642-3658.
26. Insinna C, Lu Q, Teixeira I, et al. Investigation of F-BAR domain PACSIN proteins uncovers membrane tubulation function in cilia assembly and transport. *Nat Commun.* 2019;10(1):428.
27. Hori Y, Kobayashi T, Kikyo Y, Kontani K, Katada T. Domain architecture of the atypical Arf-family GTPase Arl13b involved in cilia formation. *Biochem Biophys Res Commun.* 2008;373(1):119-124.
28. Knodler A, Feng S, Zhang J, et al. Coordination of Rab8 and Rab11 in primary ciliogenesis. *Proc Natl Acad Sci U S A.* 2010;107(14):6346-6351.
29. Sharma M, Naslavsky N, Caplan S. A role for EHD4 in the regulation of early endosomal transport. *Traffic.* 2008;9(6):995-1018.
30. Jones T, Naslavsky N, Caplan S. Eps15 homology domain protein 4 (EHD4) is required for Eps15 homology domain protein 1 (EHD1)-mediated endosomal recruitment and fission. *PLoS One.* 2020;15(9):e0239657.
31. Simone LC, Caplan S, Naslavsky N. Role of phosphatidylinositol 4,5-bisphosphate in regulating EHD2 plasma membrane localization. *PLoS One.* 2013;8(9):e74519.
32. Simone LC, Naslavsky N, Caplan S. Scratching the surface: actin' and other roles for the C-terminal Eps15 homology domain protein, EHD2. *Histol Histopathol.* 2014;29(3):285-292.
33. Bahl K, Naslavsky N, Caplan S. Role of the EHD2 unstructured loop in dimerization, protein binding and subcellular localization. *PLoS One.* 2015;10(4):e0123710.
34. Moren B, Shah C, Howes MT, et al. EHD2 regulates caveolar dynamics via ATP-driven targeting and oligomerization. *Mol Biol Cell.* 2012;23(7):1316-1329.
35. Shah C, Hegde BG, Moren B, et al. Structural insights into membrane interaction and caveolar targeting of dynamin-like EHD2. *Structure.* 2014;22(3):409-420.
36. Naslavsky N, Caplan S. C-terminal EH-domain-containing proteins: consensus for a role in endocytic trafficking, EH? *J Cell Sci.* 2005;118(Pt 18):4093-4101.
37. Grant BD, Caplan S. Mechanisms of EHD/RME-1 protein function in endocytic transport. *Traffic.* 2008;9(12):2043-2052.
38. Naslavsky N, Caplan S. EHD proteins: key conductors of endocytic transport. *Trends Cell Biol.* 2011;21(2):122-131.
39. Yeow I, Howard G, Chadwick J, et al. EHD proteins cooperate to generate Caveolar clusters and to maintain Caveolae during repeated mechanical stress. *Curr Biol.* 2017;27:2951-2962.
40. Naslavsky N, Boehm M, Backlund PS Jr, Caplan S. Rabenosyn-5 and EHD1 interact and sequentially regulate protein recycling to the plasma membrane. *Mol Biol Cell.* 2004;15(5):2410-2422.
41. Folks JL. Combination of independent tests. *Handbook of Statistics.* Vol 4. Elsevier; 1984:113-121.
42. Rice WR. A consensus combined P-value test and the family-wide significance of component tests. *Biometrics.* 1990;46(2):303-308.
43. Deo R, Kushwah MS, Kamerkar SC, et al. ATP-dependent membrane remodeling links EHD1 functions to endocytic recycling. *Nat Commun.* 2018;9(1):5187.
44. Lee DW, Zhao X, Scarselletta S, et al. ATP binding regulates oligomerization and endosome association of RME-1 family proteins. *J Biol Chem.* 2005;280:280-290.
45. Naslavsky N, Rahajeng J, Sharma M, Jovic M, Caplan S. Interactions between EHD proteins and Rab11-FIP2: a role for EHD3 in early endosomal transport. *Mol Biol Cell.* 2006;17(1):163-177.
46. Grant B, Zhang Y, Paupard MC, Lin SX, Hall DH, Hirsh D. Evidence that RME-1, a conserved C. elegans EH-domain protein, functions in endocytic recycling. *Nat Cell Biol.* 2001;3(6):573-579.
47. Lin SX, Grant B, Hirsh D, Maxfield FR. Rme-1 regulates the distribution and function of the endocytic recycling compartment in mammalian cells. *Nat Cell Biol.* 2001;3(6):567-572.
48. Bahl K, Xie S, Spagnol G, Sorgen P, Naslavsky N, Caplan S. EHD3 protein is required for tubular recycling endosome stabilization, and an asparagine-glutamic acid residue pair within its Eps15 homology (EH) domain dictates its selective binding to NPF peptides. *J Biol Chem.* 2016;291(26):13465-13478.
49. Spagnol G, Reiling C, Kieken F, Caplan S, Sorgen PL. Chemical shift assignments of the C-terminal Eps15 homology domain-3 EH domain. *Biomol NMR Assign.* 2014;8(2):263-267.
50. Kieken F, Sharma M, Jovic M, et al. Mechanism for the selective interaction of C-terminal Eps15 homology domain proteins with specific Asn-Pro-Phe-containing partners. *J Biol Chem.* 2010;285(12):8687-8694.
51. Kieken F, Jovic M, Naslavsky N, Caplan S, Sorgen PL. EH domain of EHD1. *J Biomol NMR.* 2007;39(4):323-329.
52. Kumar D, Reiter J. How the centriole builds its cilium: of mothers, daughters, and the acquisition of appendages. *Curr Opin Struct Biol.* 2021;66:41-48.
53. Nachury MV, Loktev AV, Zhang Q, et al. A core complex of BBS proteins cooperates with the GTPase Rab8 to promote ciliary membrane biogenesis. *Cell.* 2007;129(6):1201-1213.
54. Feng S, Knodler A, Ren J, et al. A Rab8 guanine nucleotide exchange factor-effector interaction network regulates primary ciliogenesis. *J Biol Chem.* 2012;287(19):15602-15609.
55. Kieken F, Jovic M, Tonelli M, Naslavsky N, Caplan S, Sorgen PL. Structural insight into the interaction of proteins containing NPF, DPF, and GPF motifs with the C-terminal EH-domain of EHD1. *Protein Sci.* 2009;18(12):2471-2479.

SUPPORTING INFORMATION

Additional supporting information may be found in the online version of the article at the publisher's website.

How to cite this article: Jones T, Naslavsky N, Caplan S. Differential requirements for the Eps15 homology domain proteins EHD4 and EHD2 in the regulation of mammalian ciliogenesis. *Traffic.* 2022;23(7):360-373. doi:[10.1111/tra.12845](https://doi.org/10.1111/tra.12845)